Frontiers in Bioscience Landmark

Front. Biosci. (Landmark Ed) **2023**; 28(11): 282
https://doi.org/10.31083/j.fbl2811282

Original Research

Endothelial Progenitor-Cell-Derived Exosomes Induced by Astragaloside IV Accelerate Type I Diabetic-wound Healing via the PI3K/AKT/mTOR Pathway in Rats

Wu Xiong[1], Xue Bai[2], Xi Zhang[3,4], Huajuan Lei[5], Hui Xiao[2], Luyao Zhang[6], Yuting Xiao[6], Qianpei Yang[6], Xiaoling Zou[2,*]

[1]Department of Burns and Plastic Surgery, the First Affiliated Hospital of Hunan University of Chinese Medicine, 410007 Changsha, Hunan, China
[2]Department of Endocrinology, the First Affiliated Hospital of Hunan University of Chinese Medicine, 410007 Changsha, Hunan, China
[3]Department of Scientific Research, Hunan Brain Hospital, 410007 Changsha, Hunan, China
[4]Clinical Medical School of Hunan University of Chinese Medicine, 410007 Changsha, Hunan, China
[5]Department of Anesthesiology, the First Affiliated Hospital of Hunan University of Chinese Medicine, 410007 Changsha, Hunan, China
[6]College of Integrated Traditional Chinese and Western Medicine, Hunan University of Chinese Medicine, 410208 Changsha, Hunan, China
*Correspondence: zxl000123@163.com (Xiaoling Zou)
Academic Editors: Luigi De Masi, Paola Bontempo and Daniela Rigano
Submitted: 23 May 2023 Revised: 15 July 2023 Accepted: 19 July 2023 Published: 8 November 2023

Abstract

Objective: We explore the effects of endothelial progenitor cell (EPC)-derived exosomes (EPCexos) and of astragaloside IV (ASIV)-stimulated EPCexos (ASIV-EPCexos) on type I diabetic-wound healing, and determine the basic molecular mechanisms of action. **Methods**: EPCs were exposed to different concentrations of ASIV to generate ASIV-EPCexos. A chronic-wound healing model involving streptozotocin-stimulated diabetic rats was established. These rats were treated with EPCexos, ASIV-EPCexos, rapamycin, and wortmannin. Wound healing was evaluated by direct photographic observation, hematoxylin and eosin staining, and Masson's trichrome staining. **Results**: ASIV treatment increased the abilities of EPCs (e.g., proliferation), as well as exosome secretion. EPCexo showed a "cup holder" like structure. Treatment with ASIV-EPCexos increased the wound-healing rate, collagen-deposition area, bromodeoxyuridine uptake, VEGF expression, and the number of CD31- and αSMA- positive cells, whereas decreased epidermal thickness and CD45 expression. The expression of the PI3K/AKT/mTOR pathway increased, whereas the expression of inflammatory factor decreased. However, rapamycin and wortmannin reversed these changes. **Conclusions**: ASIV-EPCexos may accelerate type I diabetic-wound healing via the PI3K/AKT/mTOR pathway. This study may lay the foundation for new clinical treatment options for patients with type I diabetic wounds.

Keywords: astragaloside IV; PI3K/AKT/mTOR; endothelial progenitor cells; exosome; angiogenesis

1. Introduction

The delayed and prolonged healing of diabetic wounds is a major challenge for healthcare providers worldwide [1]. Presently, typical clinical treatments for patients with chronic wounds are the dressing care of local ulcer wounds and repeated debridement of necrotic tissue [2,3]. These dressings include preservatives, antioxidants, growth factors, and analgesics [4]. However, the treatment effects are inadequate.

Exosomes, with diameters ranging from 30 to 200 nm, are extracellular vesicles originating from the endosome and contain a wide range of substances, including proteins, DNA, lipids, and metabolites [5]. The process of exosome biosynthesis includes the double inward folding of the cell membrane and the creation of intracellular multivesicular bodies (MVBs) that contain intraluminal vesicles (ILVs). These MVBs can then either be degraded through fusion with lysosomes or autophagic vesicles or release ILVs as exosomes [5,6]. Exosomes are crucial in various physiological and pathological processes via cellular communication, such as immune response, tissue repair, and cancer progression [5,7,8]. For instance, mesenchymal stem cell (MSC)-derived exosomes (MSCexo) promote the growth of endothelial cells and skin fibroblasts to accelerate the repair of skin wounds [9]. Fibroblast proliferation and endothelial-cell angiogenesis are the salient features of diabetic-wound healing [10]. Endothelial progenitor cells (EPCs) foster the regeneration of endothelial cells by secreting exosomes instead of self-differentiating into mature endothelial cells [11]. EPC-derived exosomes (EPCexos) can appreciably promote the vitality and angiogenesis of rat aortic endothelial cells [12]. Therefore, we speculate that EPCexos may be effective as a potential treatment for promoting diabetic-wound healing.

The decoction made from astragalus root is called "astragalus" and is widely used in traditional Chinese medicine to treat viral and bacterial infections, inflammation, and cancers. Astragaloside IV (ASIV) is one of the main active ingredients in the aqueous extract of astragalus [13]. ASIV has various pharmacological effects through multiple

Copyright: © 2023 The Author(s). Published by IMR Press.
This is an open access article under the CC BY 4.0 license.

Publisher's Note: IMR Press stays neutral with regard to jurisdictional claims in published maps and institutional affiliations.

pathways, including anti-inflammatory, antifibrotic, antioxidative stress, antiasthma, antidiabetic, immunological, and cardioprotective [14]. Therefore, ASIV effectively protects against focal cerebral ischemia, liver fibrosis, cancer, diabetes, and cardiovascular diseases [15]. After myocardial infarction, ASIV exerts angiogenesis and cardioprotective effects via the PTEN/PI3K/AKT pathway [16]. Our previous studies have also shown that ASIV promotes the secretion of EPCexos [17]. However, the effects of ASIV-stimulated EPCexos (ASIV-EPCexos) on diabetic-wound healing have not yet been explored.

PI3K is important in mitosis, survival, differentiation, cytoskeleton configuration and remodeling, angiogenesis, glucose transport regulation, and cyst transport [18]. PI3K catalyzes the formation of phosphatidylinositol triphosphate (PIP3), which binds to the PH domain of 3-phosphoinositide-dependent protein kinase 1 (PDK1) to activate AKT [19]. The PI3K/AKT/mTOR pathway modulates cell growth, survival, metabolism, and immunity [20,21]. Activation of the PI3K/AKT/mTOR pathway increases the expression of VEGF and stimulates angiogenesis [22]. The AKT/eNOS pathway can regulate angiogenesis and tissue repair [23]. We speculate that ASIV could promote EPCexo secretion and diabetic-wound healing via the PI3K/AKT pathway.

In the present study, animal experiments were conducted to explore the effects of ASIV-EPCexos on type I diabetic-wound healing, and determine the underlying mechanism of action.

2. Materials and Methods

2.1 Separation, Identification, and Treatment of Cells

This study was approved by the Ethics Committee of the First Hospital of Hunan University of Chinese Medicine (NO.HN-LL-KY-2020-013-01). All experiments were performed strictly in accordance with the Declaration of Helsinki, and informed consent was obtained from all the participants.

Umbilical-cord blood from healthy, full-term newborns was obtained from the Obstetrics and Gynecology Department of the First Hospital, Hunan University of Chinese Medicine, Changsha, China. Heparin (20 U/mL) was added to the cord blood for anticoagulation. The isolated cord blood mononuclear cells were resuspended in DMEM (D5796, Sigma, Saint Louis, MO, USA) with 10% FCS (04-001-1ACS, Gibco, Carlsbad, CA, USA). The cell suspension (3×10^6/mL) was inoculated into a plate with slides and cultured in an incubator (DH-160I, Shanghai Santeng, Shanghai, China) at 37 °C with 5% CO_2 and saturated humidity. The cells were identified using flow cytometry and immunofluorescence (IF) staining. Afterward, the EPCs were treated with the corresponding concentrations of ASIV (0, 50, 100, and 200 mg/L) for 72 h. As previously described [24], the exosomes were harvested by centrifugation at 200,000 $\times g$ for 60 min, and treated and examined by transmission electron microscope (TEM, JEM1400, Jeol, Beijing, China).

2.2 Animal Model

Male, 8-week-old Sprague-Dawley rats (n = 96) weighing 250–300 g were purchased from Hunan SJA Laboratory Animal Co., Ltd. (Changsha, Hunan, China). The experimental protocol was approved by the Animal Experimentation Ethics Committee of the First Hospital of Hunan University of Chinese Medicine (NO. ZYFY20201018-2). Rats were housed alone and exposed to a 12/12-h light/dark cycle at 22–24 °C and with *ad libitum* access to food and water. One week later, they were divided into control (n = 12) and diabetic (n = 84) groups. After fasting for 12–16 h, rats in the diabetic group were given a single intraperitoneal injection of streptozotocin (STZ) solution (65 mg/kg body weight, in 0.1 M citrate buffer, pH = 4.5, S0130, Sigma-Aldrich, Saint Louis, State of Missouri, USA) to induce a type I diabetes model [25,26]. Blood glucose levels were randomly monitored daily after the first 72 h. When three consecutive random blood-glucose concentrations were more than 16.7 mmol/L, a successful model of diabetes was considered to have been established. After 14 d, rats in the control and diabetic groups were anesthetized and shaved. The dorsal skin of the rats was disinfected, and four pieces of 1.5 × 1.5-cm^2 full-layer skin were removed from the deep fascia on both sides of the rat spine. All the rats were injected intraperitoneally with 100 mg/kg bromodeoxyuridine (BrdU, Sigma, St. Louis, MO, USA). STZ, rapamycin, and wortmannin were purchased from Sigma. Rats in the diabetic group were randomly divided into the following groups: an EPCexo group, a low dose of ASIV-EPCexos group (low-ASIV-EPCexo), a medium dose of ASIV-EPCexos group (mid-ASIV-EPCexo), a high dose of ASIV-EPCexos group (hi-ASIV-EPCexo), a hi-ASIV-EPCexo + rapamycin group, and a hi-ASIV-EPCexo + wortmannin group. Rats in the EPCexo group were injected with 500 mg/L EPCexos. The low-, mid-, and hi-ASIV-EPCexo groups were treated with ASIV-EPCexos at different concentrations (250, 500, and 1000 mg/L). Rats in the hi-ASIV-EPCexo + rapamycin and hi-ASIV-EPCexo + wortmannin groups were treated with rapamycin (37 nM, mTOR blocker, ab120224, AbcamCam-bridge, Cambridgeshire, UK) or wortmannin (15 µg/kg, PI3K blocker, ab120148, AbcamCam-bridge, Cambridgeshire, UK), respectively, following treatment with 1000 mg/L ASIV-EPCexos. EPCexos were locally injected around the wounds [27,28]. Wound photographs were recorded at 0, 3, 7, 10, and 14 d, and the percentage of wound healing area was calculated using the Image-Pro Plus image analysis system following skin resection. Rats were euthanized at 14 d, and the skin was excised and preserved for further analysis.

2.3 Flow Cytometry

The expression of the surface markers CD31 (+), CD34 (+), CD45 (–), and CD133 (+) of EPCs was evaluated using flow cytometry. After approximately 12 d of subculture, cells were obtained. The resuspended cells were precipitated with 100 µL of 0.5% BSA-PBS. Subsequently, 2 µL CD34-FITC (bs-0646R-FITC, Bioss, Beijing, China), 1 µL CD133-FITC (bs-0209R-FITC, Bioss, Beijing, China), 3 µL CD31-FITC (bs-0195R-FITC, Bioss, Beijing, China), and 1 µL CD45-FITC (bs-0522R-FITC, Bioss, Beijing, China) antibodies were incubated with the cells at 37 °C in the dark for 30 min. After washing and centrifugation, the cells were analyzed by flow cytometry (A00-1-1102, Beckman, Brea, California, USA).

2.4 IF Staining

The expression of CD34 and VEGF receptor 2 (VEGFR2) of EPCs was detected using IF staining. IF staining was used to evaluate the expression of CD31, αSMA, CD45, BrdU, and VEGF in the skin tissue. Paraffin-embedded skin tissue blocks were cut into 4-µm sections. These were dewaxed and rehydrated using xylene and ethanol and subsequently immersed in citrate buffer (pH 6.0) and heated to retrieve the antigens. The sections were stained with sodium borohydride solution and Sudan black and rinsed with distilled water. The slides and sections were placed in 5% BSA and incubated for 60 min. Slides and sections were incubated overnight at 4 °C with diluted primary antibodies against CD34 (ab81289, 1:50, Abcam, Cambridge, Cambridgeshire, UK), VEGFR2 (ab39378, 1:50, Abcam, Cambridge, Cambridgeshire, UK), CD31 (11265-1-AP, 1:100, PTG, Wuhan, Hubei, China), αSMA (55135-1-AP, 1:100, PTG, Wuhan, Hubei, China), CD45 (ab33923, 1:100, Abcam, Cambridge, Cambridgeshire, UK), BrdU (#5292, 1:100, CST, Danvers, Massachusetts, USA), and VEGF (ab46154, 1:100, Abcam, Cambridge, Cambridgeshire, UK). The next day, the slides and sections were incubated at 37 °C for 90 min with anti-rabbit or mouse IgG (SA00013-4 or SA00013-1, 1:200, Proteintech, Chicago, Illinois, USA). Slides and sections were incubated with 4′,6-diamidino-2-phenylindole and observed using a fluorescence microscope.

2.5 Cell Counting kit-8 (CCK-8)

Following treatment of EPCs with ASIV for 24 h, the medium was removed, discarded, and replaced with 100 µL medium containing 10% CCK8 (NU679, Dojindo, Kumamoto, Japan). The absorbance was measured at 450 nm using a microplate reader (MB-530, HEALES, Shenzhen, Guangdong, China).

2.6 Transwell Assay

Intervention EPCs were hydrolyzed into single cells. A cell suspension, prepared in a serum-free basal medium (1×10^5/mL), was added to the upper Transwell chamber (33318035, Corning, Corning, NY, USA). A medium with 10% FBS was then added to the lower chamber. After 48 h, the medium was discarded, and the cells in the upper compartment were cleaned. The cells in the lower compartment were fixed with a 1:1 acetone–methanol solution for 20 min. The cells were stained and subsequently photographed using an inverted microscope (DSZ2000X, Cnmicro, Beijing, China).

2.7 Tube Formation Assay

Corning Matrigel Basement Membrane Matrix (356234, BD Biosciences, Franklin Lakes, NJ, USA) was added to each well of a 48-well plate until the wells were evenly covered without bubbles. The 48-well plates were then incubated at 37 °C for 1 h. Cells were digested with 0.25% trypsin and suspended before the addition of 7.5×10^4 cells/well to the 48-well plate. Photographs were taken (100× magnification) after incubation at 37 °C for 6 h.

2.8 Enzyme-Linked Immunosorbent Assay (ELISA)

An ExoQuantTM Overall Exosome Capture and Quantification Assay Kit (#K1201-100, Biovision, San Francisco, CA, USA) was used for quantitative analysis of exosomes. All procedures were carried out following the guidelines. The absorbance was obtained at 450 nm. The concentration of the exosomes was calculated after plotting a standard curve.

2.9 Western Blotting (WB)

A 30 µg sample of denatured protein was added to each well of the gel. Samples were electrophoresed for 130 min at a constant voltage of 75 V. Target proteins were transferred from the gel to a nitrocellulose (NC) membrane at a constant current of 300 mA. Following the transfer process, the NC membrane was subjected to blocking. The primary antibodies against CD63 (25682-1-AP), CD9 (20597-1-AP), CD81 (66866-1-Ig), mTOR (66888-1-Ig), ras homolog enriched in brain (Rheb, 15924-1-AP), PI3K (67071-1-Ig), AKT (10176-2-AP), PIP3 (17552-1-AP), PDK1 (10026-1-AP), and β-actin (60008-1-Ig) were purchased from Proteintech (Chicago, Illinois, USA), whereas those against VEGFa (ab46154), VEGFb (ab185696), VEGFc (ab9546), fibroblast growth factor (FGF, ab208687), and angiotensin-1 (Ang-1, ab183701), p-mTOR (ab109268), eNOS (ab76198), and tuberous sclerosis 2 (TSC2, ab32554) were purchased from Abcam (Cambridge, Cambridgeshire, UK). The primary antibody was incubated overnight at 4 °C. The NC membrane was incubated with anti-mouse/rabbit IgG (SA00001-1 or SA00001-2, Proteintech, Chicago, Illinois, USA) for 90 min. Protein bands were visualized by SuperECL Plus hypersensitive luminescent solution (K-12045-D50, Advansta, Beijing, China). Photographs were taken using a ChemiScope 6100 chemiluminescence imaging system (CLINX, Shanghai, China).

2.10 Hematoxylin and Eosin (HE) Staining

HE staining was used to observe the morphological changes in rat skin. Paraffin-embedded rat-skin tissue samples were cut into 4-µm-thick sections using a slicer. The sections were dewaxed and rehydrated using xylene and ethanol and stained with HE. The sections were examined under a microscope (BA210T, Motic, Xiamen, Fujian, China).

2.11 Masson's Trichrome (MT) Staining

Paraffin-embedded rat skin tissues were cut, dewaxed, and rehydrated. The sections were incubated with hematoxylin solution, rinsed with distilled water, and stained with acid fuchsin solution. Next, the sections were then incubated with 1% phosphomolybdic acid and blue aniline solutions for 5 min. The samples were examined under a microscope.

2.12 Reverse Transcription-Quantitative PCR (RT-qPCR)

Total RNA was extracted, and the cDNA was obtained by reverse transcription (CW2569, Beijing CWBIO Co., Ltd., Beijing, China). The primer sequences for the target genes are presented in Table 1. Primers were synthesized by Shanghai Sangon Biotech. A PCR system containing the fluorescent dye UltraSYBR Mixture (CW2601, Beijing CWBIO Co., Ltd., Beijing, China) was prepared, and the reaction was performed with QuantStudio1 (Thermo, Waltham, Massachusetts, USA). The fluorescence signal was monitored in real time, and the internal reference was β-actin. The gene levels were calculated ($2^{-\Delta\Delta Ct}$ method).

Table 1. Reverse transcription-quantitative polymerase chain reaction (RT-qPCR) primer sequences.

Gene	Sequences (5′-3′)
VEGFa	F: GGGAGCAGAAAGCCCATGAA
	R: GCTGGCTTTGGTGAGGTTTG
VEGFb	F: GTGGTCAAACAACTCGTGCC
	R: CTGGGGCTGTCTGGCTTC
VEGFc	F: AACCTCCATGTGTGTCCGTC
	R: TGCTGAGGTAACCTGTGCTG
FGF	F: ACACCACGGACAAAGAAATTGAGG
	R: CCCGATAGAATTACCCGCCAAGCA
Ang-1	F: ACATCCCGTCTTGAAATCCAAC
	R: TGTCCAGCTCTTCCTTGTGT
mTOR	F: AGAACCAATTATACTCGCTCCCT
	R: GCAACCTCAAAGCAGTCCCC
Rheb	F: GGACCTGCATATGGAAAGGGT
	R: CATCACCGAGCACGAAGACT
eNOS	F: GTTGACCAAGGCAAACCACC
	R: GCTGACTCCCTCCCAGTCTA
PI3K	F: AGCCACAGATCCACTTAACCC
	R: CTTGCTGTCCCCACTTTACTGA
AKT	F: GTCACCTCTGAGACCGACACC
	R: GCCTCCGTTCACTGTCCAC
PDK1	F: CGCCTCTATGCACAGTACTTCCAG
	R: CGTCAGCCTCGTGGTTGGTTC
TSC2	F: TACCCCTGAGAAGGACAAGTT
	R: CAAGCTGGCACTGGTAAGAGA
PIP3	F: GCAGTTTGAACCCAAAGCCC
	R: AAGCGCATTCCTTTCCGTTG
IL-6	F: TCACTATGAGGTCTACTCGG
	R: CATATTGCCAGTTCTTCGTA
IL-1β	F: CAGCAGCATCTCGACAAGAG
	R: AAAGAAGGTGCTTGGGTCCT
β-actin	F: ACCCTGAAGTACCCCATCGAG
	R: AGCACAGCCTGGATAGCAAC

2.13 Statistical Analysis

Statistical analyses were conducted using GraphPad Prism 8.0.1 (GraphPad Software, Inc., San Diego, CA, USA), and the data were expressed as mean ± standard deviation. The differences between the two groups were analyzed utilizing the Student's *t*-test. For comparing differences among multiple groups, a one-way analysis of variance (ANOVA) was performed, followed by a Tukey post-hoc test. Statistical significance was set at $p < 0.05$.

3. Results

3.1 ASIV Promotes EPCs Proliferation, Migration, and Tube-Formation Abilities

EPCs were identified using flow cytometry and IF staining. The expression of CD31, CD34, and CD133 was positive, but the expression of CD45 was negative, indicating that the endothelial cells were successfully extracted (**Supplementary Fig. 1**). As depicted in Fig. 1A, the viability of EPCs in the 50, 100, and 200 mg/L groups exhibited a substantial enhancement in comparison to the control group. The cell migration and tube-formation abilities of EPCs in the 50, 100, and 200 mg/L groups were appreciably improved (Fig. 1B,C). EPCs in the 100 mg/L group showed optimal ability. Therefore, ASIV promotes the progress of EPCs, and a concentration of 100 mg/L exhibited the optimal effect.

3.2 ASIV Promotes EPCexo Secretion

We next examined the effect of ASIV on EPCexo secretion. The EPCexo characteristic markers CD9, CD63, and CD81 levels were detected [17]. The expression of those markers was positive in all the groups (Fig. 2A), indicating the successful extraction of EPCexos. In TEM, EPCexos showed a "cup holder" structure in the four groups (Fig. 2B). EPCexos were quantified using ELISA. As shown in Fig. 2C, the concentration of EPCexos was appreciably higher in the 50, 100, and 200 mg/L groups than in the control group, with the highest concentration observed in the 100 mg/L group. These findings indicate that ASIV facilitates EPCexo secretion, with the optimal effect observed at a concentration of 100 mg/L.

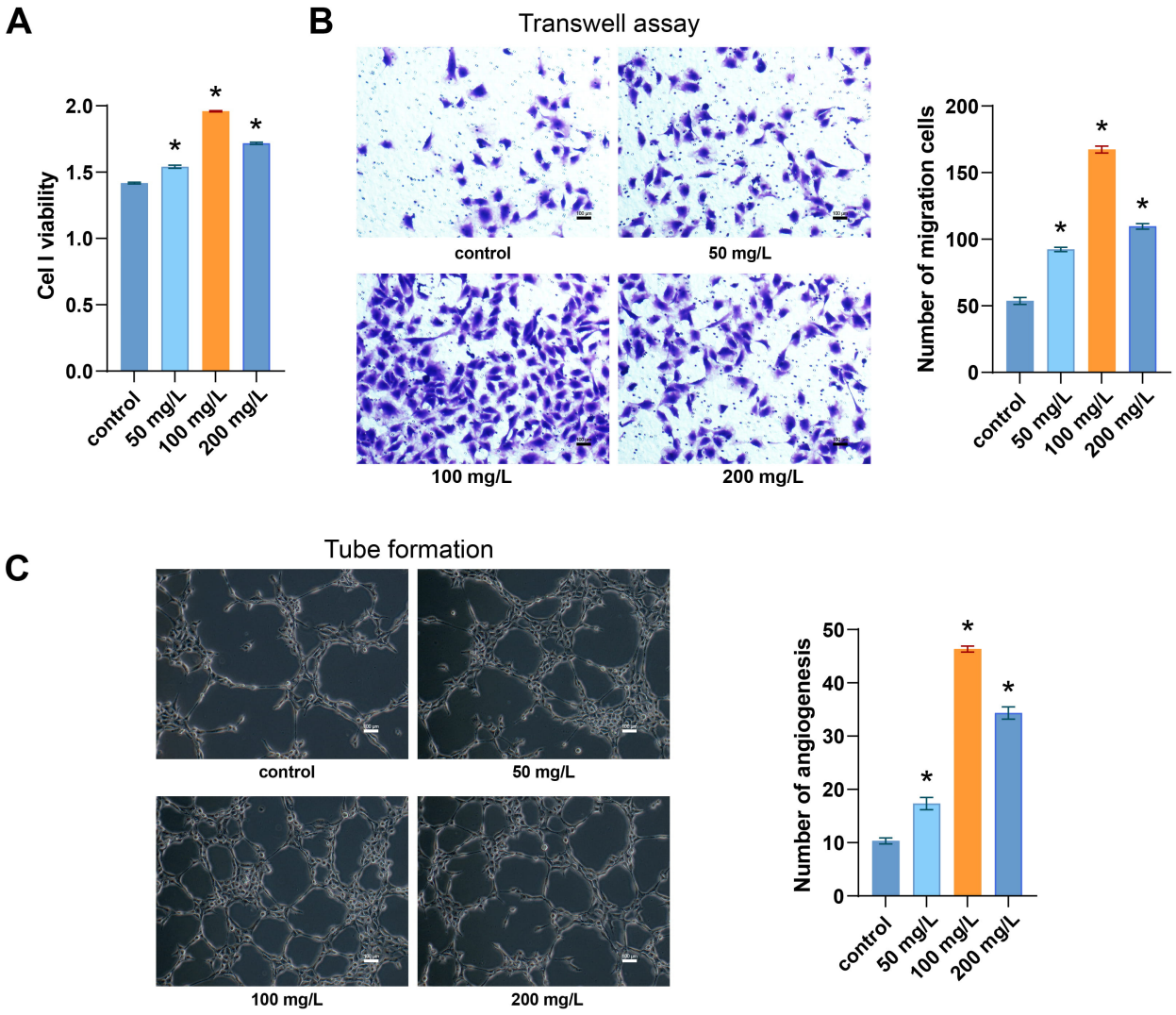

Fig. 1. ASIV promotes EPC progress. (A) Representative graphs of CCK-8 showing cell viability. (B) Representative light micrographs and graphs showing cell migration by Transwell assay. (C) Representative light micrographs and graphs of tube formation assay revealing the tube formation ability. *$p < 0.05$ vs the control group. Magnification = 100×, scale bar = 100 µm. ASIV, astragaloside IV; EPC, endothelial progenitor cell; CCK-8, cell counting kit-8.

3.3 ASIV-EPCexos Promote Type I Diabetic-Wound Healing

The chronic-wound model in STZ-stimulated diabetic rats was used to investigate whether ASIV-EPCexos promote type I diabetic-wound healing. The EPCexo group exhibited a higher rate of wound healing compared to the model group (Fig. 3A,B). After ASIV-EPCexo treatment, wound healing rates in the low-, mid-, and hi-ASIV-EPCexo groups were substantially higher than in the EPCexo group, and the hi-ASIV-EPCexo group exhibited optimal healing. As opposed to the model group, the positive staining rates of BrdU and VEGF were substantially raised in the EPCexo group (Fig. 3C–E). Moreover, the low-, mid- and hi-ASIV-EPCexo groups exhibited stronger positive staining for BrdU and VEGF compared to the EPCexo group, and the hi-ASIV-EPCexo group demonstrated the highest staining intensity. Granulation tissue formation, epithelial reformation, collagen deposition, fibroblast proliferation, and angiogenesis are hallmarks of wound healing [29]. In contrast to the model group, the epidermal thickness in the EPCexo and low-, mid-, and hi-ASIV-EPCexo groups gradually decreased. The collagen area was higher in the low-, mid-, and hi-ASIV-EPCexo groups than in the model group (Fig. 4A–C). IF staining results revealed that the number (No.) of CD31 and αSMA positive cells were raised in the EPCexo and low-, mid-, and hi-ASIV-EPCexo groups (Fig. 4D–G). Rapamycin and wortmannin reversed the above changes in the hi-ASIV-EPCexo group. In conclusion, ASIV-EPCexo accelerated skin-wound healing in diabetic rats, with 1000 mg/L ASIV-EPCexo showing an optimal effect.

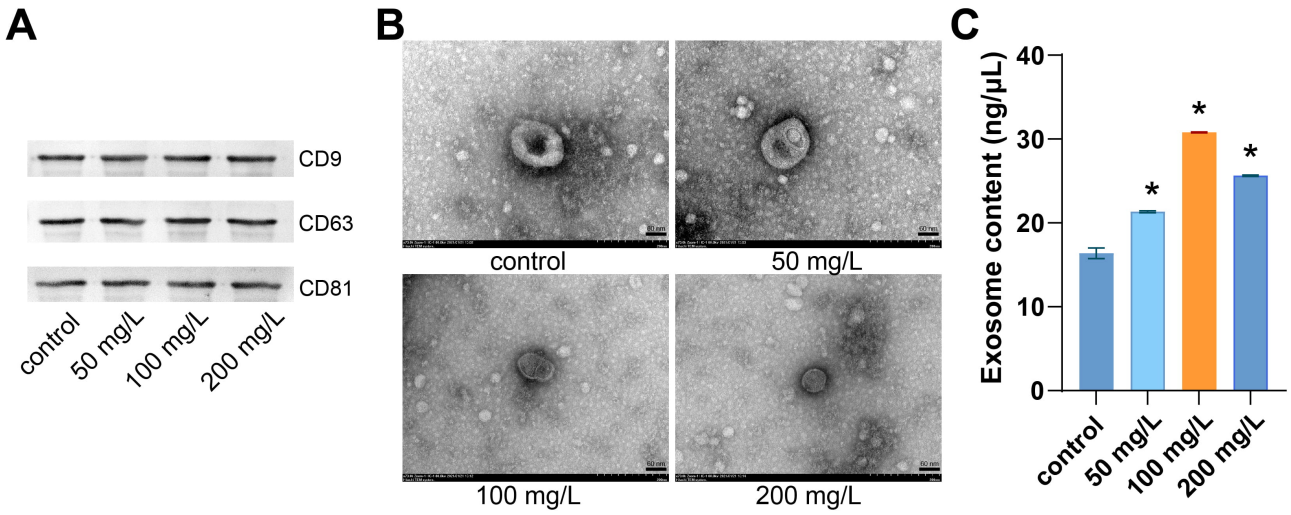

Fig. 2. ASIV promotes EPCexo secretion. (A) The WB analysis of shows the expression of EPCexo characteristic markers CD9, CD63, and CD81. (B) Representative micrographs of EPCexo morphology were obtained via TEM. Scale bar = 60 nm. (C) Comparison of EPCexo content via ELISA in the different groups. *$p < 0.05$ vs the control group. EPCexo, EPC-derived exosomes; WB, western blotting; ELISA, enzyme-linked immunosorbent assay; TEM, transmission electron microscope.

3.4 ASIV-EPCexos Promote Angiogenesis via the PI3K/AKT/mTOR Pathway in Diabetic-Wounds

To study the mechanism by which ASIV-EPCexos accelerate type I diabetic wound healing, we analyzed the changes in skin tissue at the molecular level. The expression levels related to vascular growth (*VEGFa*, *VEGFb, VEGFc*, *FGF*, and *Ang-1*) in the EPCexo group were higher than in the model group. These expression levels were further increased following ASIV-EPCexo treatment. Compared to the hi-ASIV-EPCexo group, these expression levels in the hi-ASIV-EPCexo + rapamycin and hi-ASIV-EPCexo + wortmannin groups were substantially decreased (Fig. 5A,B). We then examined the expression levels of the pathway proteins and genes in the samples. In terms of the model group, the expression levels of p-mTOR, *mTOR*, p-mTOR/mTOR, *Rheb*, *eNOS*, *PI3K*, *AKT*, *PIP3*, *PDK1*, and *TSC2* in the EPCexo group were raised (Fig. 5C–F), although several of them were not substantially different. In addition, the expression levels of genes and proteins related to these pathways were higher in the low-, mid-, and hi-ASIV-EPCexo groups than in the EPCexo group. However, the expression of these genes and proteins decreased in the hi-ASIV-EPCexo + rapamycin and hi-ASIV-EPCexo + wortmannin groups. The results suggest that ASIV-EPCexos may activate the PI3K/AKT/mTOR pathway, thereby promoting angiogenesis.

3.5 ASIV-EPCexos Inhibit Inflammation via the PI3K/AKT/mTOR Pathway in Diabetic-Wounds

Interleukin (IL)-1β-dependent inflammation and immunity have important healing effects in diabetic wounds [30,31]. Therefore, we next investigated the expression of inflammatory factors and immune cells in the skin of diabetic wounds. As shown in Fig. 6A, the expression levels of the *IL-6* and *IL-1*β genes were lower in the EPCexo group than in the model group. Furthermore, their expression in the low-, mid-, and hi-ASIV-EPCexo groups was even lower than in the EPCexo group. However, their expression was higher in the hi-ASIV-EPCexo + rapamycin and hi-ASIV-EPCexo + wortmannin groups than in the hi-ASIV-EPCexo group. IF staining analysis revealed that the number of CD45 immune cells was lower in the EPCexo group than in the model group (Fig. 6B,C). The CD45 immune cell content was lower in the low-, mid-, and hi-ASIV-EPCexo groups compared to the EPCexo group, whereas the rapamycin and wortmannin inhibitors reversed this effect. These results suggest that ASIV-EPCexos inhibit inflammation in skin wounds through the PI3K/AKT/mTOR pathway.

4. Discussion

The present work found that ASIV-EPCexos promoted type I diabetic-wound healing, which could be blocked by the mTOR- and PI3K- specific inhibitors, rapamycin, and wortmannin. We found that ASIV-EPCexos promoted type I diabetic wound healing by activating the PI3K/AKT/mTOR pathway. Our earlier study only demonstrated that ASIV could stimulate human EPCs to secrete exosomes [17], whereas the present study examined the effects of ASIV-EPCexos on wound healing in type I diabetic rats. We established a type I diabetic rat model with skin wounds and treated with EPCexos or with low-, mid-, or high-ASIV-EPCexos. Photographs of the wound healing at different time points showed all of these treatments promoted the healing of diabetic wounds. Following treatment

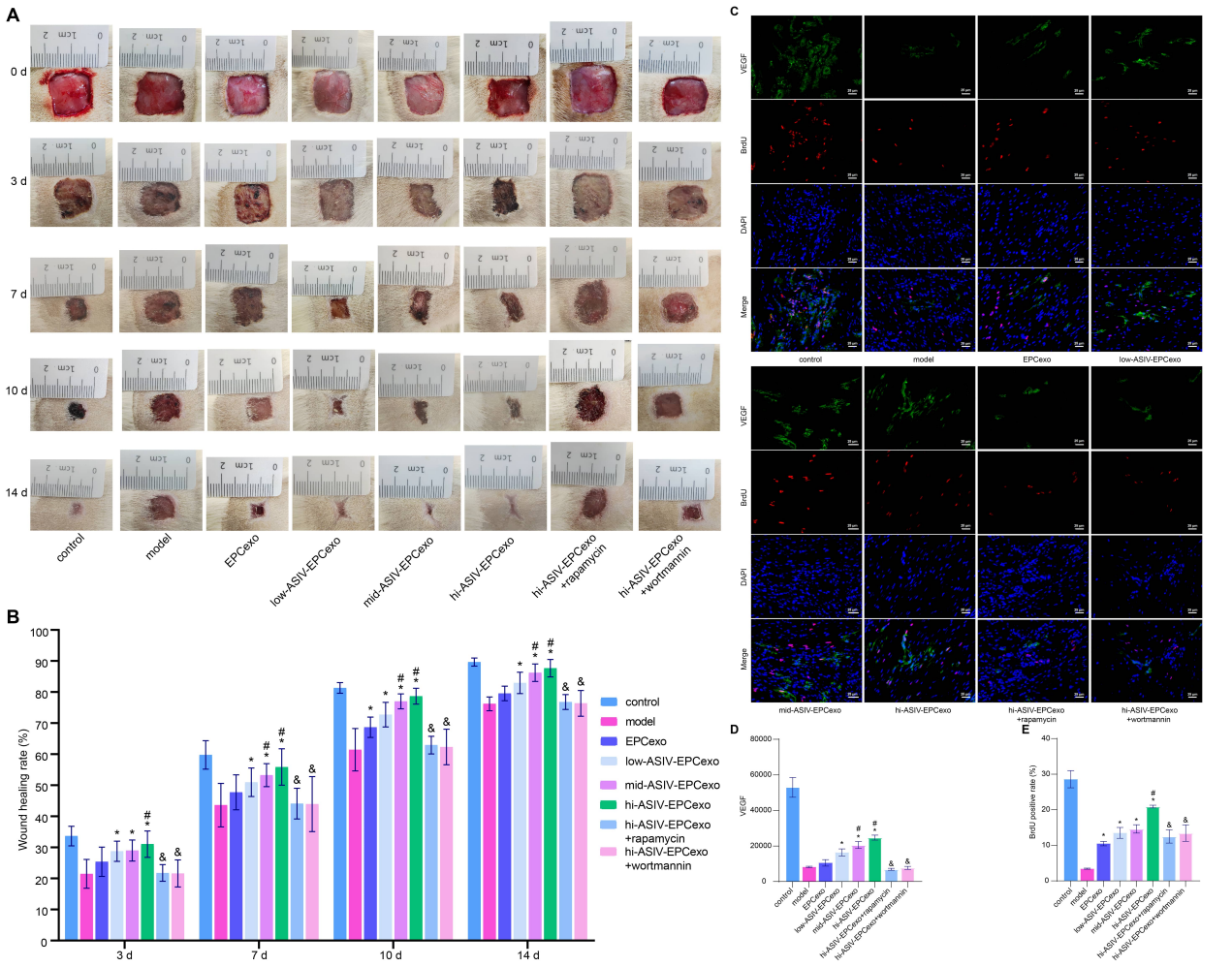

Fig. 3. ASIV-EPCexos may promote type I diabetic-wound healing via facilitating BrdU and VEGF expression. (A) Representative images of the diabetic wounds of rat skin at different time points. (B) Comparison of wound healing rate of rat skin at different time points. (C) Representative micrographs of IF staining showing the expression of BrdU and VEGF. (D,E) Statistical analysis of the expression of BrdU and VEGF. *$p < 0.05$ vs the model group. #$p < 0.05$ vs the EPCexo group. &$p < 0.05$ vs the hi-ASIV-EPCexo group. Magnification = 400×, scale bar = 25 µm. n = 12 rats/group. IF, immunofluorescence; BrdU, bromodeoxyuridine; hi-ASIV-EPCexo, a high dose of ASIV-EPCexos.

with EPCexos or ASIV-EPCexos, the expression of inflammatory factors decreased, the levels of VEGF, BrdU, CD31, and αSMA increased, and the VEGF/PI3K/AKT/mTOR pathway was activated. In addition, IF staining showed that treatment with EPCexos or ASIV-EPCexos reduced the expression of CD45. However, rapamycin and wortmannin were able to reverse these changes. In summary, ASIV-EPCexo treatment promoted diabetic-wound healing by activating the PI3K/AKT/mTOR pathway.

The growth factor VEGF has important angiogenic activity that promotes mitosis and inhibits apoptosis of endothelial cells, as well as promoting vascular permeability and cell migration [32]. ASIV enhances the expression of VEGF, thereby promoting angiogenesis in wound tissues [33]. CD31 is involved in immune regulation and angiogenesis [34]. The downregulation of miR-126-3p in parathyroid tumors promotes endothelial cell transition to the αSMA mesenchymal phenotype and increases VEGFA expression, thereby affecting angiogenesis [35]. Xu *et al.* [36] reported that miR-221-3p in EPCexo can accelerate skin-wound healing in diabetic mice. The present study used histological and molecular experiments to show that ASIV-EPCexos promoted diabetic-wound healing, consistent with the results of previous studies.

FGF regulates cell fate, angiogenesis, immunity, and metabolism via its receptors FGFR1, FGFR2, FGFR3, and FGFR4 [37]. Ang-1 plays a regulatory role in processes associated with proliferation, inflammation, vascular fibrosis, and remodeling [38]. We found that ASIV-EPCexos increased the expression of genes and proteins related to blood-vessel growth (VEGFa, VEGFb, VEGFc, FGF, and Ang-1), which could explain their ability to promote an-

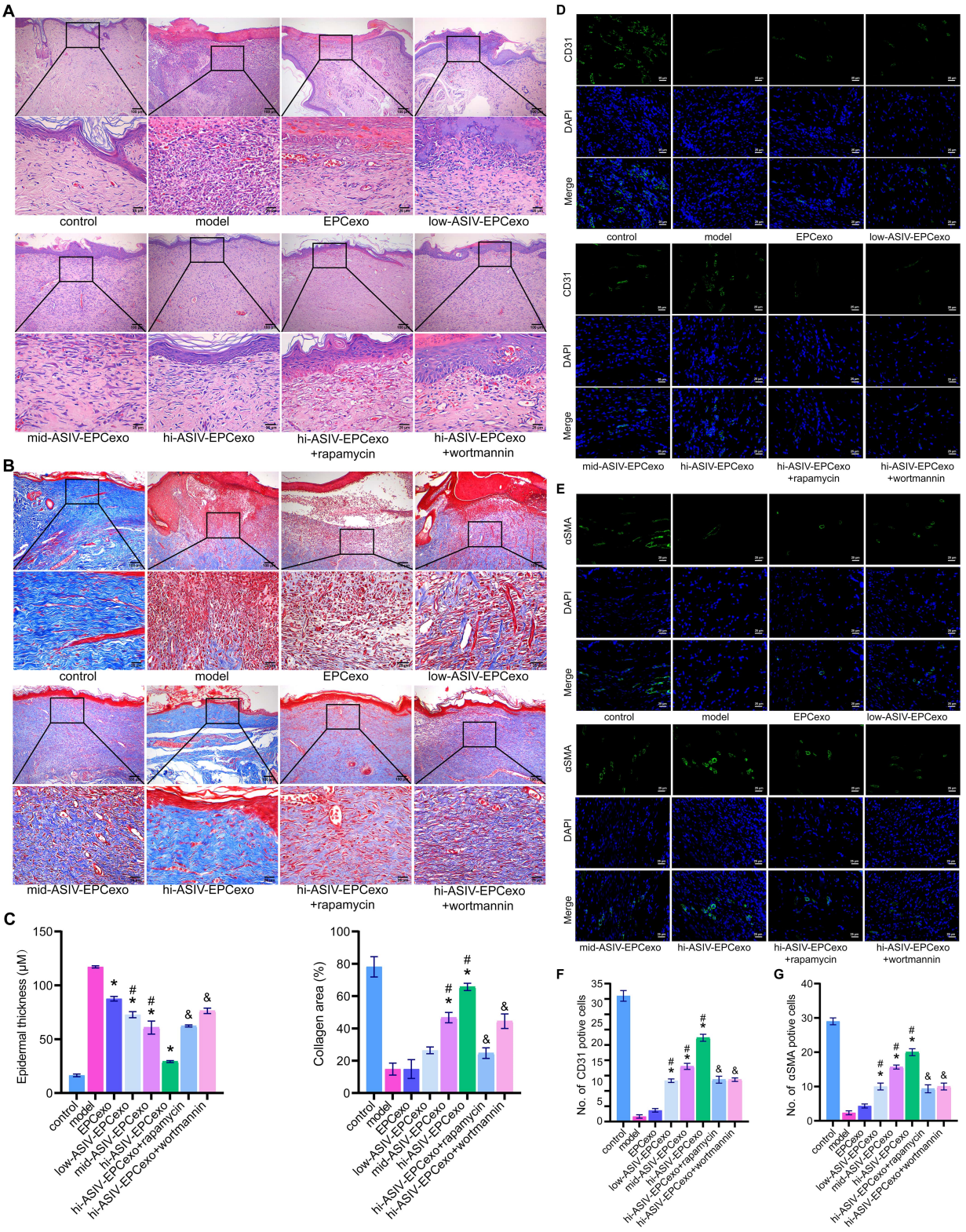

Fig. 4. ASIV-EPCexos may promote type I diabetic-wound healing via modulating CD31 and αSMA expression. (A) Representative micrographs of HE staining. (B) Representative micrographs of MT staining. (C) Statistical analysis of (A,B). (D,E) Representative micrographs of IF staining showing CD31 and αSMA expression. (F,G) Statistical analysis of (D,E). *$p < 0.05$ vs the model group. #$p < 0.05$ vs the EPCexo group. &$p < 0.05$ vs the hi-ASIV-EPCexo group. Magnification = 100× or 400×, scale bar = 100 μm or 25 μm. n = 12 rats/group. HE, hematoxylin and eosin; MT, masson's trichrome.

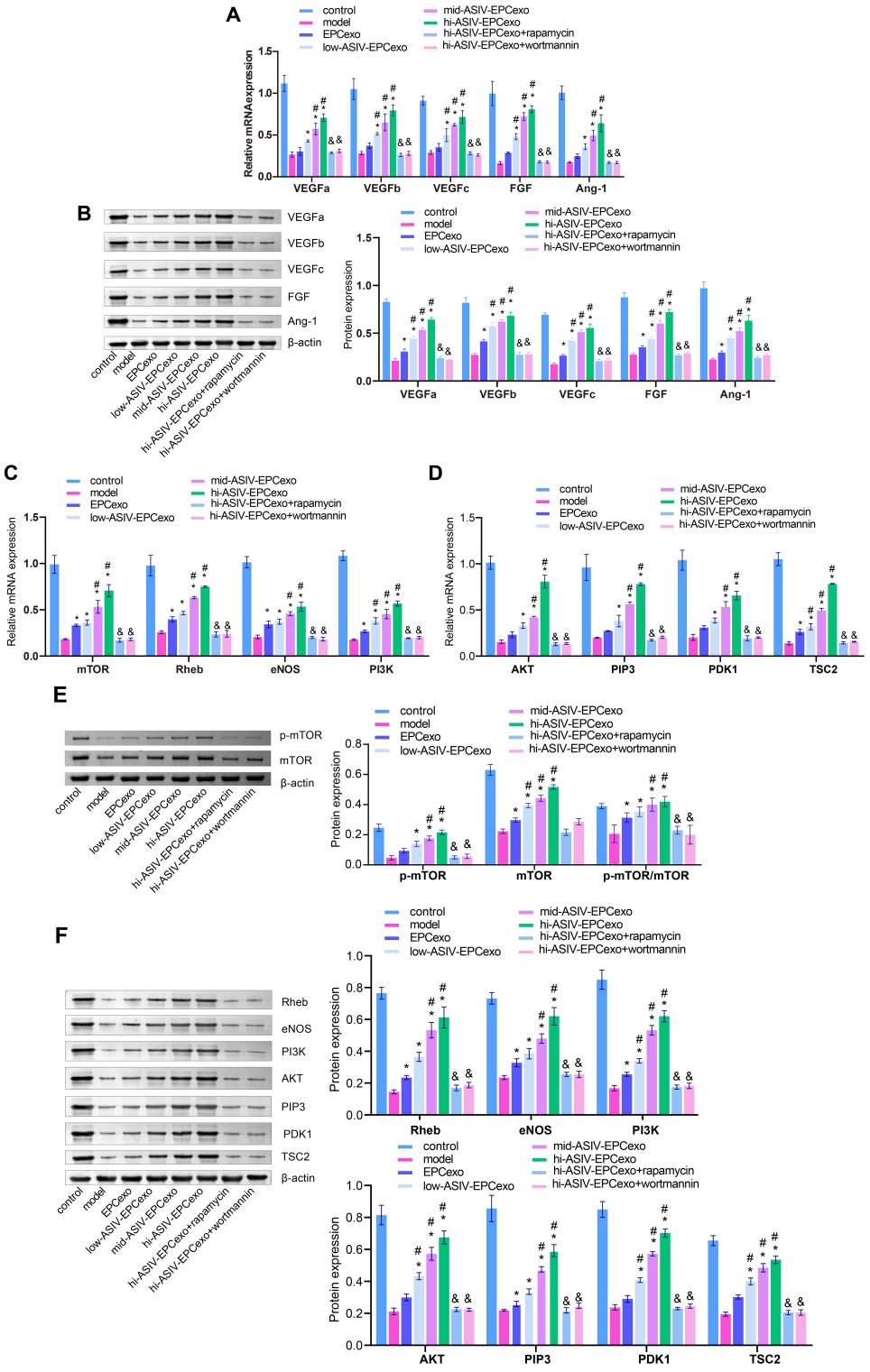

Fig. 5. ASIV-EPCexos promote angiogenesis via the PI3K/AKT/mTOR pathway in diabetic wounds. (A) Representative graphs of RT-qPCR showing the relative mRNA expression of *VEGFa*, *VEGFb*, *VEGFc*, *FGF*, and *Ang-1*. (B) The WB analysis shows the protein expression of VEGFa, VEGFb, VEGFc, FGF, and Ang-1. (C,D) Representative graphs of RT-qPCR showing the expression of *mTOR*, *Rheb*, *eNOS*, *PI3K*, *AKT*, *PIP3*, *PDK1*, and *TSC2*. (E) The WB analysis shows the protein expression of mTOR and p-mTOR. (F) The WB analysis shows the protein expression of Rheb, eNOS, PI3K, AKT, PIP3, PDK1, and TSC2. *$p < 0.05$ vs the model group. #$p < 0.05$ vs the EPCexo group. &$p < 0.05$ vs the hi-ASIV-EPCexo group. n = 12 rats/group. FGF, fibroblast growth factor; Ang-1, angiotensin-1; Rheb, ras homolog enriched in brain; PIP3, phosphatidylinositol triphosphate; PDK1, PH domain of 3-phosphoinositide-dependent protein kinase 1; TSC2, tuberous sclerosis 2.

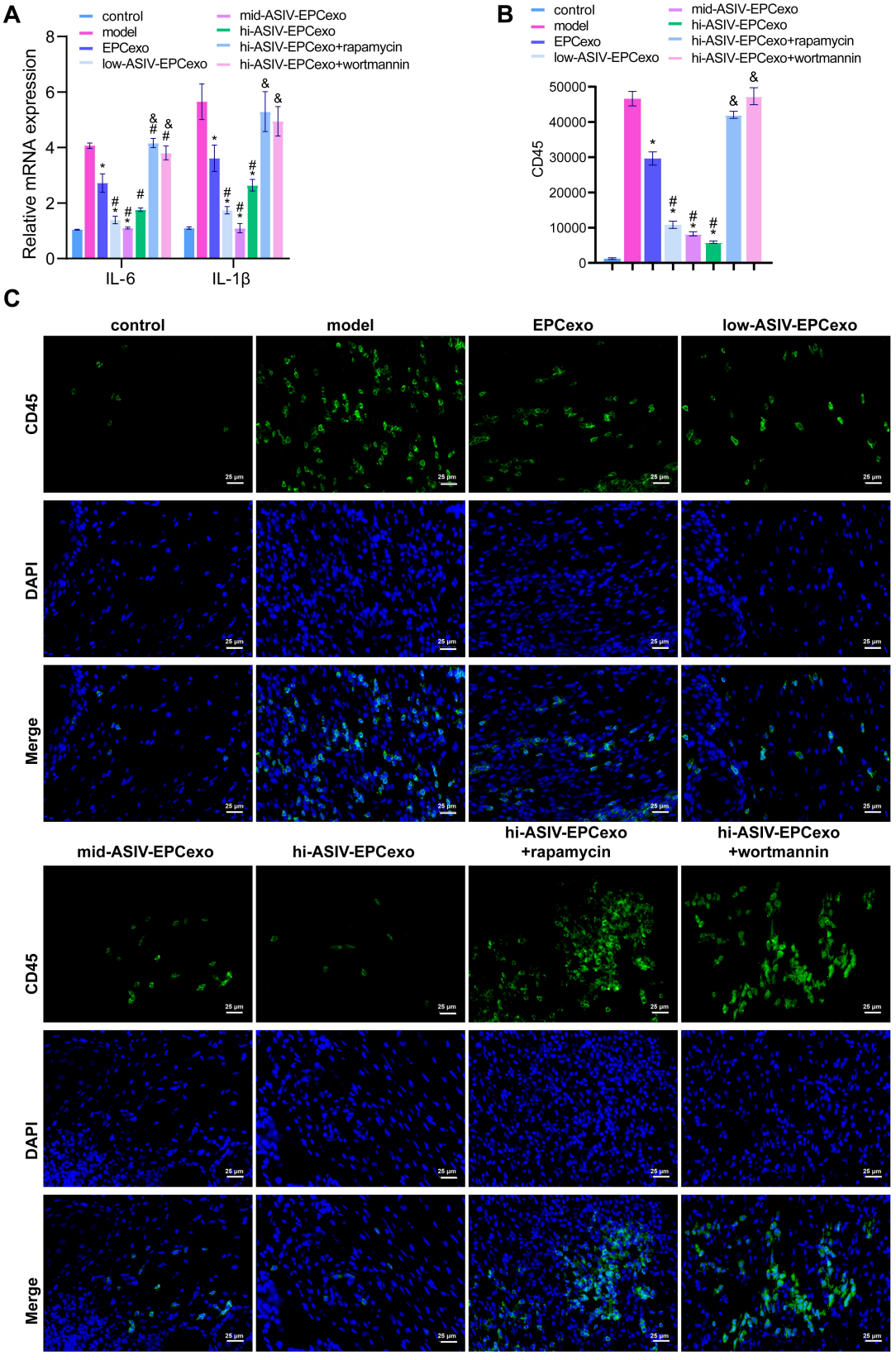

Fig. 6. ASIV-EPCexos inhibit inflammation via the PI3K/AKT/mTOR pathway in type I diabetic-wound healing. (A) Representative graphs of RT-qPCR showing the mRNA expression of *IL-6* and *IL-1β*. (B,C) Representative micrographs and statistical analysis of CD45 immune cells. *$p < 0.05$ vs the model group. #$p < 0.05$ vs the EPCexo group. &$p < 0.05$ vs the hi-ASIV-EPCexo group. Magnification = 400×, scale bar = 25 μm. n = 12 rats/group.

giogenesis in diabetic wounds. Many substances regulate the proliferation, migration, and tube-forming abilities of EPCs via the PI3K/AKT pathway, including naringin [39]. AKT-dependent TSC2 phosphorylation promotes RHEB-mTORC1 [40]. TSC2/Rheb mediates extracellular signal-regulated, kinase-dependent regulation of mTORC1 activity in C2C12 myoblasts [41]. Downstream targets of the PI3K/AKT pathway, mTOR and eNOS, can increase VEGF expression and promote angiogenesis [42,43]. The current study found that the expression of genes and proteins related to the PI3K/AKT/mTOR pathway was significantly increased following treatment with ASIV-EPCexos, and this was reversed by rapamycin and wortmannin. In short, our results indicate that ASIV-EPCexos can activate the PI3K/AKT/mTOR pathway and promote angiogenesis at the wound surface by targeting mTOR and eNOS in endothelial cells.

Chronic, unresolved inflammation is a hallmark of non-healing wounds and adversely affects the wound-healing process [44]. The pro-inflammatory cytokines IL-6 and IL-1β are key mediators in the disrupted pathophysiology of osteoarthritis [45]. CD45 cells contribute to the inflammatory response by expressing granulocyte-macrophage colony-stimulating factors, key inflammatory cytokines, and transcription factors [46]. Zhou *et al*. [47] showed that ASIV could effectively reduce placental oxidative stress and inflammatory-cytokine production in gestational diabetes. In the present study, treatment of a rat model with ASIV-EPCexos decreased the levels of *IL-6*, *IL-1β,* and CD45 cells in the skin tissue, with rapamycin and wortmannin reversing these effects. The current findings suggest that ASIV-EPCexos activate the PI3K/AKT/mTOR pathway, thereby inhibiting the inflammatory response in diabetic wounds.

Type I diabetes mellitus (TIDM) is an autoimmune disease in which the immune system mistakenly attacks and destroys insulin-producing β-cells in the pancreas, leading to an absolute insulin deficiency, resulting in hyperglycemia [48]. Currently, the etiology of TIDM is believed to be associated with genetic and environmental (e.g., viral infections) factors [48,49]. Type II diabetes mellitus (TIIDM), a metabolic disease, is characterized by elevated blood glucose levels caused by either insulin resistance or insufficient insulin secretion. The resulting hyperglycemia puts additional pressure on β-cells to compensate for the increased demand for insulin secretion. Consequently, this may deplete β-cells, resulting in a gradual decline in β-cell function and leading to insulin deficiency, ultimately causing diabetes [50]. The development of TIIDM is commonly associated with genetics, lifestyle, and insulin resistance, such as a sedentary lifestyle, poor diet, and obesity [51]. The objective of this study was to examine the impact of ASIV-EPCexos on wound healing in TIDM and explore the underlying mechanisms of action.

Diabetic foot ulcers (DFU) are a significant and grave complication of diabetes. They are characterized by impaired blood supply to the feet caused by neuropathy or vascular disease, which subsequently leads to ulceration, infection, and a range of other complications [52]. DFU has emerged as a global public health concern with serious implications for human well-being due to its unfavorable prognosis, ultimately increasing the risk of ulceration, amputation, and even mortality [52,53]. DFU primarily occurs in adults with TIIDM but can also occur in adult patients with TIDM [54–56]. For example, a retrospective study by Rasmussen *et al*. [54] reported that out of 5640 adult patients with TIDM, 255 developed DFU. Among 6953 adult patients with TIIDM, 310 developed DFU in a specialty hospital in Denmark during 2001–2014. In a prospective clinical study, among 31 adult patients diagnosed with DFU, 14 were caused by TIDM [56]. There are also a number of studies focusing on wound healing in TIDM [31,57,58]. For example, Liu *et al*. [31] found that neutrophil extracellular traps (NETs) contribute to NLRP3 inflammasome activation and sustained inflammatory responses in type I diabetic wounds. Costa *et al*. [57] revealed that xanthohumol effectively regulates inflammation, oxidative stress, and angiogenesis in the process of cutaneous wound healing in rats with TIDM. White *et al*. [58] conducted a study to investigate the efficacy of combination therapies involving various growth factors in promoting wound healing using a mouse model of type I diabetic wounds. Their findings showed that triple therapy was highly effective [58]. This study aimed to investigate the effects and potential mechanisms of ASIV-EPCexos on a rat model of type I diabetic-wound healing. After skin excision, we performed HE, MT, and IF staining (VEGF, BrdU, CD31, αSMA, and CD45). The expression levels of VEGFa, VEGFb, VEGFc, FGF, Ang-1, p-mTOR, mTOR, p-mTOR/mTOR, Rheb, eNOS, PI3K, AKT, PIP3, PDK1, and TSC2 were detected by RT-qPCR and WB. In addition, we also detected the expression of IL-6 and IL-1β. The current results illustrated that in rats, ASIV-EPCexos accelerated type I diabetic-wound healing via the PI3K/AKT/mTOR pathway. This study may lay the foundation for the development of new potential clinical therapeutic agents for TIDM patients with DFU.

There are similarities in the underlying causes of impaired and delayed wound healing in patients with TIDM and TIIDM. Chronic hyperglycemia, a key common factor, leads to a persistent state of inflammation that disrupts the natural progression of inflammation, repair, and regeneration during wound healing [57,59,60]. Additionally, compromised immune function in patients with TIDM and TIIDM increases the vulnerability of wounds to infections and elongates the healing process. Notably, the dysfunction of immune cells and foot neuropathy contributes to the formation of DFU and further hinder the healing process [59–61]. In the current study, the expression levels of the IL-6 and IL-1β genes in the EPCexo group were decreased compared

with the model group. IF staining analysis revealed that the number of CD45 immune cells in the EPCexo group was lower than that in the model group. The inhibitors rapamycin and wortmannin reversed the effects (Fig. 6). These results suggest that ASIV-EPCexos inhibit inflammation in wounded skin through the PI3K/AKT/mTOR pathway. Therefore, we speculated that ASIV-EPCexos might also be a potential drug to alleviate wound healing in TIIDM. However, the effect of ASIV-EPCexos on wound healing in TIIDM and its mechanism have not been explored in depth, which is a limitation of the current study. In future studies, we anticipate investigating the effects and mechanisms of ASIV-EPCexos on wound healing in TIIDM by constructing a rat model.

Several cell types, such as MSCs, fibroblasts, macrophages, and EPCs, have been reported to play roles in wound healing [10,62–65]. For example, MSCs or MSCexos can promote wound healing [62,63]. Fibroblast proliferation and endothelial cell angiogenesis are prominent features of diabetic wound healing [10]. Our previous studies have demonstrated that ASIV has the potential to enhance the secretion of exosomes from EPCs. This was determined by comparing the mass concentration of exosomes secreted by EPCs in both the control group and the group treated with ASIV [17]. EPCs possess remarkable migratory capacity and the ability to differentiate into endothelial cells, making them crucial in neovascularization, tissue regeneration, and wound healing processes [65]. Huang *et al*. [66] reported that ASIV-treated EPCs had a positive impact on angiogenesis and wound healing. EPCs promote endothelial cell regeneration by the secretion of exosomes [11]. Specifically, ASIV-EPCexos have been observed to appreciably enhance the proliferation, migration, and angiogenesis of rat aortic endothelial cells [12]. Therefore, ASIV-EPCexos were chosen as the focus of the study.

Exosomes contain various biologically active components, including proteins, lipids, and RNA. Multiple mechanisms may be responsible for mediating the therapeutic effects of exosomes. The proangiogenic and anti-inflammatory effects of the active components of EPCexos remain unclear, and a future goal should be to identify these molecules.

5. Conclusions

The current study confirms the stimulatory effect of ASIV on EPCexo secretion. ASIV-EPCexos promote diabetic-wound healing by activating the PI3K/AKT/mTOR pathway. These results may provide novel therapeutic options for the clinical treatment of diabetic wounds.

Availability of Data and Materials

The datasets used and analyzed during the current study are available from the corresponding author on reasonable request.

Author Contributions

WX and XZo designed the research study. WX, XB, XZh, HL, HX, LZ, and YX performed the research. QY analyzed the data. WX wrote the manuscript. All authors contributed to editorial changes in the manuscript. All authors read and approved the final manuscript.

Ethics Approval and Consent to Participate

This study was approved by the Ethics Committee of the First Hospital of Hunan University of Chinese Medicine (NO.HN-LL-KY-2020-013-01). All experiments were performed strictly in accordance with the Declaration of Helsinki, and informed consent was obtained from all the participants.

Acknowledgment

Not applicable.

Funding

This research was funded by the Clinical Medical Technology Innovation Guidance Project of Hunan Provincial Science and Technology Department (No. 2021SK51412), the Hunan Natural Science Foundation Youth Fund Project (No. 2019J50460), the National Natural Science Foundation of China Youth Science Fund Project (No. 81904217), and Science and Health Joint Project of Hunan Natural Science Foundation (No.2021JJ70033).

Conflict of Interest

The authors declare no conflict of interest.

Supplementary Material

Supplementary material associated with this article can be found, in the online version, at https://doi.org/10.31083/j.fbl2811282.

References

[1] Zheng SJ, Jia CY. Present status of research in bone marrow-derived mesenchymal stem cells for promoting the healing of diabetic ulcer. Zhonghua Shao Shang Za Zhi. 2012; 28: 291–293. (In Chinese)

[2] Eldor R, Raz I, Ben Yehuda A, Boulton AJM. New and experimental approaches to treatment of diabetic foot ulcers: a comprehensive review of emerging treatment strategies. Diabetic Medicine: a Journal of the British Diabetic Association. 2004; 21: 1161–1173.

[3] Zarei F, Negahdari B, Eatemadi A. Diabetic ulcer regeneration: stem cells, biomaterials, growth factors. Artificial Cells, Nanomedicine, and Biotechnology. 2018; 46: 26–32.

[4] Sami DG, Abdellatif A, Azzazy HME. Turmeric/oregano formulations for treatment of diabetic ulcer wounds. Drug Development and Industrial Pharmacy. 2020; 46: 1613–1621.

[5] Pegtel DM, Gould SJ. Exosomes. Annual Review of Biochemistry. 2019; 88: 487–514.

[6] Mashouri L, Yousefi H, Aref AR, Ahadi AM, Molaei F, Alahari SK. Exosomes: composition, biogenesis, and mechanisms in

cancer metastasis and drug resistance. Molecular Cancer. 2019; 18: 75.
[7] Yan W, Jiang S. Immune Cell-Derived Exosomes in the Cancer-Immunity Cycle. Trends in Cancer. 2020; 6: 506–517.
[8] Girón J, Maurmann N, Pranke P. The role of stem cell-derived exosomes in the repair of cutaneous and bone tissue. Journal of Cellular Biochemistry. 2022; 123: 183–201.
[9] Shi R, Jin Y, Hu W, Lian W, Cao C, Han S, *et al*. Exosomes derived from mmu_circ_0000250-modified adipose-derived mesenchymal stem cells promote wound healing in diabetic mice by inducing miR-128-3p/SIRT1-mediated autophagy. American Journal of Physiology. Cell Physiology. 2020; 318: C848–C856.
[10] Huang X, Liang P, Jiang B, Zhang P, Yu W, Duan M, *et al*. Hyperbaric oxygen potentiates diabetic wound healing by promoting fibroblast cell proliferation and endothelial cell angiogenesis. Life Sciences. 2020; 259: 118246.
[11] Yue Y, Wang C, Benedict C, Huang G, Truongcao M, Roy R, *et al*. Interleukin-10 Deficiency Alters Endothelial Progenitor Cell-Derived Exosome Reparative Effect on Myocardial Repair via Integrin-Linked Kinase Enrichment. Circulation Research. 2020; 126: 315–329.
[12] Yi M, Wu Y, Long J, Liu F, Liu Z, Zhang YH, *et al*. Exosomes secreted from osteocalcin-overexpressing endothelial progenitor cells promote endothelial cell angiogenesis. American Journal of Physiology. Cell Physiology. 2019; 317: C932–C941.
[13] Zang Y, Wan J, Zhang Z, Huang S, Liu X, Zhang W. An updated role of astragaloside IV in heart failure. Biomedicine & Pharmacotherapy. 2020; 126: 110012.
[14] Li L, Hou X, Xu R, Liu C, Tu M. Research review on the pharmacological effects of astragaloside IV. Fundamental & Clinical Pharmacology. 2017; 31: 17–36.
[15] Zhang J, Wu C, Gao L, Du G, Qin X. Astragaloside IV derived from Astragalus membranaceus: A research review on the pharmacological effects. Advances in Pharmacology (San Diego, Calif.). 2020; 87: 89–112.
[16] Cheng S, Zhang X, Feng Q, Chen J, Shen L, Yu P, *et al*. Astragaloside IV exerts angiogenesis and cardioprotection after myocardial infarction via regulating PTEN/PI3K/Akt signaling pathway. Life Sciences. 2019; 227: 82–93.
[17] Xiong W, Bai X, Xiao H, Lan HW, Zhu CH, Zhao SQ, *et al*. Effects of Astragaloside IV on exosome secretion and its microRNA-126 expression in human endothelial progenitor cells. Zhonghua Shao Shang Za Zhi. 2020; 36: 1183–1190. (In Chinese)
[18] De Santis MC, Gulluni F, Campa CC, Martini M, Hirsch E. Targeting PI3K signaling in cancer: Challenges and advances. Biochimica et Biophysica Acta. Reviews on Cancer. 2019; 1871: 361–366.
[19] Hofler A, Nichols T, Grant S, Lingardo L, Esposito EA, Gridley S, *et al*. Study of the PDK1/AKT signaling pathway using selective PDK1 inhibitors, HCS, and enhanced biochemical assays. Analytical Biochemistry. 2011; 414: 179–186.
[20] Pompura SL, Dominguez-Villar M. The PI3K/AKT signaling pathway in regulatory T-cell development, stability, and function. Journal of Leukocyte Biology. 2018. (online ahead of print)
[21] Hua H, Kong Q, Zhang H, Wang J, Luo T, Jiang Y. Targeting mTOR for cancer therapy. Journal of Hematology & Oncology. 2019; 12: 71.
[22] Chen J, Zhang X, Liu X, Zhang C, Shang W, Xue J, *et al*. Ginsenoside Rg1 promotes cerebral angiogenesis via the PI3K/Akt/mTOR signaling pathway in ischemic mice. European Journal of Pharmacology. 2019; 856: 172418.
[23] Icli B, Wu W, Ozdemir D, Li H, Cheng HS, Haemmig S, *et al*. MicroRNA-615-5p Regulates Angiogenesis and Tissue Repair by Targeting AKT/eNOS (Protein Kinase B/Endothelial Nitric Oxide Synthase) Signaling in Endothelial Cells. Arteriosclerosis, Thrombosis, and Vascular Biology. 2019; 39: 1458–1474.
[24] Lian Q, Xu J, Yan S, Huang M, Ding H, Sun X, *et al*. Chemotherapy-induced intestinal inflammatory responses are mediated by exosome secretion of double-strand DNA via AIM2 inflammasome activation. Cell Research. 2017; 27: 784–800.
[25] Lu CH, Ou HC, Day CH, Chen HI, Pai PY, Lee CY, *et al*. Deep sea minerals ameliorate diabetic-induced inflammation via inhibition of TNFα signaling pathways. Environmental Toxicology. 2020; 35: 468–477.
[26] Hanna R, Nour-Eldine W, Saliba Y, Dagher-Hamalian C, Hachem P, Abou-Khalil P, *et al*. Cardiac Phosphodiesterases Are Differentially Increased in Diabetic Cardiomyopathy. Life Sciences. 2021; 283: 119857.
[27] Hu Y, Tao R, Chen L, Xiong Y, Xue H, Hu L, *et al*. Exosomes derived from pioglitazone-pretreated MSCs accelerate diabetic wound healing through enhancing angiogenesis. Journal of Nanobiotechnology. 2021; 19: 150.
[28] Yang J, Chen Z, Pan D, Li H, Shen J. Umbilical Cord-Derived Mesenchymal Stem Cell-Derived Exosomes Combined Pluronic F127 Hydrogel Promote Chronic Diabetic Wound Healing and Complete Skin Regeneration. International Journal of Nanomedicine. 2020; 15: 5911–5926.
[29] Gourishetti K, Keni R, Nayak PG, Jitta SR, Bhaskaran NA, Kumar L, *et al*. Sesamol-Loaded PLGA Nanosuspension for Accelerating Wound Healing in Diabetic Foot Ulcer in Rats. International Journal of Nanomedicine. 2020; 15: 9265–9282.
[30] Dai J, Shen J, Chai Y, Chen H. IL-1β Impaired Diabetic Wound Healing by Regulating MMP-2 and MMP-9 through the p38 Pathway. Mediators of Inflammation. 2021; 2021: 6645766.
[31] Liu D, Yang P, Gao M, Yu T, Shi Y, Zhang M, *et al*. NLRP3 activation induced by neutrophil extracellular traps sustains inflammatory response in the diabetic wound. Clinical Science (London, England: 1979). 2019; 133: 565–582.
[32] Melincovici CS, Boşca AB, Şuşman S, Mărginean M, Mihu C, Istrate M, *et al*. Vascular endothelial growth factor (VEGF) - key factor in normal and pathological angiogenesis. Romanian Journal of Morphology and Embryology. 2018; 59: 455–467.
[33] Luo X, Huang P, Yuan B, Liu T, Lan F, Lu X, *et al*. Astragaloside IV enhances diabetic wound healing involving upregulation of alternatively activated macrophages. International Immunopharmacology. 2016; 35: 22–28.
[34] Caligiuri G. CD31 as a Therapeutic Target in Atherosclerosis. Circulation Research. 2020; 126: 1178–1189.
[35] Verdelli C, Forno I, Morotti A, Maggiore R, Mari G, Vicentini L, *et al*. miR-126-3p contributes to parathyroid tumor angiogenesis. Endocrine-related Cancer. 2021; 28: 53–63.
[36] Xu J, Bai S, Cao Y, Liu L, Fang Y, Du J, *et al*. miRNA-221-3p in Endothelial Progenitor Cell-Derived Exosomes Accelerates Skin Wound Healing in Diabetic Mice. Diabetes, Metabolic Syndrome and Obesity: Targets and Therapy. 2020; 13: 1259–1270.
[37] Katoh M. Therapeutics Targeting FGF Signaling Network in Human Diseases. Trends in Pharmacological Sciences. 2016; 37: 1081–1096.
[38] Zhang Z, Chen L, Zhong J, Gao P, Oudit GY. ACE2/Ang-(1-7) signaling and vascular remodeling. Science China. Life Sciences. 2014; 57: 802–808.
[39] Zhao Z, Ma X, Ma J, Sun X, Li F, Lv J. Naringin enhances endothelial progenitor cell (EPC) proliferation and tube formation capacity through the CXCL12/CXCR4/PI3K/Akt signaling pathway. Chemico-biological Interactions. 2018; 286: 45–51.
[40] Chiang YJ, Liao WT, Ho KC, Wang SH, Chen YG, Ho CL, *et al*. CBAP modulates Akt-dependent TSC2 phosphorylation to promote Rheb-mTORC1 signaling and growth of T-cell acute lymphoblastic leukemia. Oncogene. 2019; 38: 1432–1447.
[41] Miyazaki M, Takemasa T. TSC2/Rheb signaling mediates ERK-

dependent regulation of mTORC1 activity in C2C12 myoblasts. FEBS Open Bio. 2017; 7: 424–433.
[42] Karar J, Maity A. PI3K/AKT/mTOR Pathway in Angiogenesis. Frontiers in Molecular Neuroscience. 2011; 4: 51.
[43] Zhan B, Xu Z, Zhang Y, Wan K, Deng H, Wang D, *et al*. Nicorandil reversed homocysteine-induced coronary microvascular dysfunction via regulating PI3K/Akt/eNOS pathway. Biomedicine & Pharmacotherapy. 2020; 127: 110121.
[44] Sawaya AP, Stone RC, Brooks SR, Pastar I, Jozic I, Hasneen K, *et al*. Deregulated immune cell recruitment orchestrated by FOXM1 impairs human diabetic wound healing. Nature Communications. 2020; 11: 4678.
[45] Kapoor M, Martel-Pelletier J, Lajeunesse D, Pelletier JP, Fahmi H. Role of proinflammatory cytokines in the pathophysiology of osteoarthritis. Nature Reviews. Rheumatology. 2011; 7: 33–42.
[46] Ahmad SF, Ansari MA, Nadeem A, Bakheet SA, Al-Ayadhi LY, Alasmari AF, *et al*. Involvement of CD45 cells in the development of autism spectrum disorder through dysregulation of granulocyte-macrophage colony-stimulating factor, key inflammatory cytokines, and transcription factors. International Immunopharmacology. 2020; 83: 106466.
[47] Zhou L, Zhang R, Yang S, Zhang Y, Shi D. Astragaloside IV alleviates placental oxidative stress and inflammation in GDM mice. Endocrine Connections. 2020; 9: 939–945.
[48] Norris JM, Johnson RK, Stene LC. Type 1 diabetes-early life origins and changing epidemiology. The Lancet. Diabetes & Endocrinology. 2020; 8: 226–238.
[49] DiMeglio LA, Evans-Molina C, Oram RA. Type 1 diabetes. Lancet (London, England). 2018; 391: 2449–2462.
[50] Carlsson S. Etiology and Pathogenesis of Latent Autoimmune Diabetes in Adults (LADA) Compared to Type 2 Diabetes. Frontiers in Physiology. 2019; 10: 320.
[51] Zheng Y, Ley SH, Hu FB. Global aetiology and epidemiology of type 2 diabetes mellitus and its complications. Nature Reviews. Endocrinology. 2018; 14: 88–98.
[52] Dixon D, Edmonds M. Managing Diabetic Foot Ulcers: Pharmacotherapy for Wound Healing. Drugs. 2021; 81: 29–56.
[53] Kerr M, Barron E, Chadwick P, Evans T, Kong WM, Rayman G, *et al*. The cost of diabetic foot ulcers and amputations to the National Health Service in England. Diabetic Medicine: a Journal of the British Diabetic Association. 2019; 36: 995–1002.
[54] Rasmussen A, Almdal T, Anker Nielsen A, Nielsen KE, Jørgensen ME, Hangaard S, *et al*. Decreasing incidence of foot ulcer among patients with type 1 and type 2 diabetes in the period 2001-2014. Diabetes Research and Clinical Practice. 2017; 130: 221–228.
[55] Huang Q, Yan P, Xiong H, Shuai T, Liu J, Zhu L, *et al*. Extracorporeal Shock Wave Therapy for Treating Foot Ulcers in Adults with Type 1 and Type 2 Diabetes: A Systematic Review and Meta-Analysis of Randomized Controlled Trials. Canadian Journal of Diabetes. 2020; 44: 196–204.e3.
[56] Frykberg RG, Gibbons GW, Walters JL, Wukich DK, Milstein FC. A prospective, multicentre, open-label, single-arm clinical trial for treatment of chronic complex diabetic foot wounds with exposed tendon and/or bone: positive clinical outcomes of viable cryopreserved human placental membrane. International Wound Journal. 2017; 14: 569–577.
[57] Costa R, Negrão R, Valente I, Castela Â, Duarte D, Guardão L, *et al*. Xanthohumol modulates inflammation, oxidative stress, and angiogenesis in type 1 diabetic rat skin wound healing. Journal of Natural Products. 2013; 76: 2047–2053.
[58] White MJV, Briquez PS, White DAV, Hubbell JA. VEGF-A, PDGF-BB and HB-EGF engineered for promiscuous super affinity to the extracellular matrix improve wound healing in a model of type 1 diabetes. NPJ Regenerative Medicine. 2021; 6: 76.
[59] Singh K, Agrawal NK, Gupta SK, Sinha P, Singh K. Increased expression of TLR9 associated with pro-inflammatory S100A8 and IL-8 in diabetic wounds could lead to unresolved inflammation in type 2 diabetes mellitus (T2DM) cases with impaired wound healing. Journal of Diabetes and its Complications. 2016; 30: 99–108.
[60] Yu T, Gao M, Yang P, Liu D, Wang D, Song F, *et al*. Insulin promotes macrophage phenotype transition through PI3K/Akt and PPAR-γ signaling during diabetic wound healing. Journal of Cellular Physiology. 2019; 234: 4217–4231.
[61] Asfour HZ, Alhakamy NA, Ahmed OAA, Fahmy UA, El-Moselhy MA, Rizg WY, *et al*. Amitriptyline-Based Biodegradable PEG-PLGA Self-Assembled Nanoparticles Accelerate Cutaneous Wound Healing in Diabetic Rats. Pharmaceutics. 2022; 14: 1792.
[62] Guillamat-Prats R. The Role of MSC in Wound Healing, Scarring and Regeneration. Cells. 2021; 10: 1729.
[63] Liu W, Yu M, Xie D, Wang L, Ye C, Zhu Q, *et al*. Melatonin-stimulated MSC-derived exosomes improve diabetic wound healing through regulating macrophage M1 and M2 polarization by targeting the PTEN/AKT pathway. Stem Cell Research & Therapy. 2020; 11: 259.
[64] Louiselle AE, Niemiec SM, Zgheib C, Liechty KW. Macrophage polarization and diabetic wound healing. Translational Research: the Journal of Laboratory and Clinical Medicine. 2021; 236: 109–116.
[65] Short WD, Steen E, Kaul A, Wang X, Olutoye OO, 2nd, Vangapandu HV, *et al*. IL-10 promotes endothelial progenitor cell infiltration and wound healing via STAT3. FASEB Journal: Official Publication of the Federation of American Societies for Experimental Biology. 2022; 36: e22298.
[66] Huang NC, Dai LG, Kang LY, Huang NC, Fu KY, Hsieh PS, *et al*. Beneficial Effects of Astragaloside IV-Treated and 3-Dimensional-Cultured Endothelial Progenitor Cells on Angiogenesis and Wound Healing. Annals of Plastic Surgery. 2021; 86: S3–S12.